Title: Redox potential as a master variable controlling pathways of metal reduction by *Geobacter sulfurreducens*

Running Title: Fe(III) reduction by *G. sulfurreducens*

Authors: Caleb E. Levar[1], Colleen L. Hoffman[2], Aubrey J. Dunshee[2], Brandy M. Toner[2, 3], Daniel R. Bond[1]

Author Affiliations: 1) BioTechnology Institute, Department of Microbiology, University of Minnesota - Twin Cities, St. Paul, MN 55108, USA
2) Department of Earth Sciences, University of Minnesota – Twin Cities, Minneapolis, MN, 55455, USA
3) Department of Soil, Water, and Climate, University of Minnesota – Twin Cities, St. Paul, MN 55108, USA

Corresponding Author:
Daniel R. Bond
140 Gortner Laboratory
1479 Gortner Ave
St. Paul, MN 55108
dbond@umn.edu

Conflict of Interest Statement: The authors declare no conflict of interest.

Keywords: Metal reduction, Extracellular electron transfer, Iron oxide, *Geobacter*

Abstract:

Geobacter sulfurreducens uses at least two different pathways to transport electrons out of the inner membrane quinone pool before reducing acceptors beyond the outer membrane. When growing on electrodes poised at oxidizing potentials, the CbcL-dependent pathway operates at or below redox potentials of -0.10 V vs. the Standard Hydrogen Electrode (SHE), while the ImcH-dependent pathway operates only above this value. Here, we provide evidence that *G. sulfurreducens* also requires different electron transfer proteins for reduction of a wide range of Fe(III)- and Mn(IV)- (oxyhydr)oxides, and must transition from a high- to low-potential pathway during reduction of commonly studied minerals. Freshly precipitated Fe(III)-(oxyhydr)oxides could not be reduced by mutants lacking the high potential pathway. Aging these minerals by autoclaving did not change their powder X-ray diffraction pattern, but restored reduction by mutants lacking the high-potential pathway. Mutants lacking the low-potential, CbcL-dependent pathway had higher growth yields with Fe(III). Together, these data suggest that the ImcH-dependent pathway exists to harvest additional energy when conditions permit, and CbcL allows respiration closer to thermodynamic equilibrium conditions. With evidence of multiple pathways within a single organism, the study of extracellular respiration should consider not only the crystal structure or solubility of a mineral electron acceptor, but rather the redox potential, as this variable determines the energetic reward affecting reduction rates, extents, and final microbial growth yields in the environment.

Introduction:

Fe(III)-(oxyhydr)oxides can exist in at least 15 mineral forms that have variable physiochemical properties and span a wide range of formal oxidation-reduction (redox) midpoint potentials (Majzlan, Navrotsky, & Schwertmann, 2004; Majzlan, 2011, 2012; Nealson & Saffarini, 1994; Schwertmann & Cornell, 2000; Thamdrup, 2000). The electron-accepting potential of any given Fe(III)-(oxyhydr)oxide structure is not a fixed value, and becomes less favorable with increasing crystallinity, particle size, pH, or ambient Fe(II) concentration (Majzlan, 2012; Navrotsky, Mazeina, & Majzlan, 2008; Sander, Hofstetter, & Gorski, 2015; Thamdrup, 2000). Differences in effective redox potential alter the energy available to be captured by bacteria able to couple the oxidation of an electron donor to reduction of these minerals (Thauer, Jungermann, Decker, & Pi, 1977). Because of this structural and environmental diversity, organisms able to reduce metals could sense the energy available in their electron acceptors and utilize different electron transfer pathways, similar to how *E. coli* uses distinct terminal oxidases in response to levels of available oxygen (Green & Paget, 2004; Russell & Cook, 1995).

One well-studied dissimilatory metal reducing organism, *Geobacter sulfurreducens*, can grow via reduction of metal (oxyhydr)oxides ranging in predicted midpoint redox potential from +0.35 V vs. the Standard Hydrogen Electrode (SHE)(e.g., birnessite, ca. $Na_xMn_{2-x}(IV)Mn(III)_xO_4$, x ~ 0.4) to -0.17 V vs. SHE (e.g., goethite, α-FeOOH) (Caccavo et al., 1994; Majzlan et al., 2004; Majzlan, 2012; Post & Veblen, 1990; Thamdrup, 2000). Recent work examining electron transfer from *G. sulfurreducens* to poised graphite electrodes demonstrated that this organism uses at least two different inner membrane electron transfer pathways, known as the CbcL- and ImcH-dependent pathways (Levar, et al., 2014; Zacharoff, et al., 2016). The 'low' potential, CbcL-dependent pathway, is required for growth with electrodes at or below potentials of -0.10 V vs. SHE, while the 'high' potential, ImcH-dependent pathway, is essential when electrodes are poised at redox potentials above this value. As mutants lacking each pathway only

grow with electrodes poised above or below these thresholds, cells containing only CbcL or ImcH could be used as 'sensors' to report the redox potential of an extracellular electron acceptor.

The discovery of multiple inner membrane pathways is based on work with electrodes held at constant potentials, but poses many questions regarding *G. sulfurreducens'* interactions with more complex mineral substrates. Does the organism transition from one pathway to the other as simple environmental factors such as Fe(II):Fe(III) ratios alter redox potentials? Do manipulations known to alter redox potential, such as pH or particle size, also influence the pathway utilized? As this +/- 0.5 V redox potential range represents nearly 50 kJ per mol of electrons transferred, do different electron transfer mechanisms allow higher yield of this microbe?

Here, we demonstrate that *G. sulfurreducens* requires both the CbcL- and the ImcH-dependent electron transfer pathways for complete reduction of a variety of Fe and Mn minerals. By using mutants only able to function at specific redox potentials, we show that minerals often used for study of extracellular electron transfer begin as 'high' potential electron acceptors reducible by the ImcH-dependent pathway, but transition during reduction to 'low' potential electron acceptors requiring the CbcL-dependent pathway. Simple variations in mineral handling such as autoclaving, or 0.5 unit pH changes that alter redox potential by 30 mV, can alter the electron transfer pathway required by the organism, further showing that bacteria detect subtle changes in mineral redox potentials. These data highlight the complexity of studying growth with minerals, and suggests that the proteins used for electron flow out of *G. sulfurreducens* are more strongly influenced by redox potential than the crystal structure, aggregation behavior, or even solubility of the terminal acceptor.

Materials and methods:

Bacterial strains and culture conditions: Strains of *Geobacter sulfurreducens* used in this study are described in Table 1. All strains were routinely cultured from freezer stocks stored at -80 degrees Celsius, and single colony picks from agar plates were used to initiate all experiments. Strains were cultured in NB minimal medium composed of 0.38 g/L KCl, 0.2 g/L NH_4Cl, 0.069 g/L $NaH_2PO_4{\cdot}H_2O$, 0.04 g/L $CaCl_2{\cdot}2H_2O$, and 0.2 g/L $MgSO_4{\cdot}7H_2O$. 10 ml/L of a chelated mineral mix containing 1.5g/L NTA, 0.1 g/L $MnCl_2{\cdot}4H_2O$, 0.3 g/L $FeSO_4{\cdot}7H_2O$, 0.17 g/L $CoCl_2{\cdot}6H2O$, 0.1 g/L $ZnCl_2$, 0.04 g/L $CuSO_4{\cdot}5H2O$, 0.005 g/L $AlK(SO_4)_2{\cdot}12H_2O$, 0.005g/L H_3BO_3, 0.09 g/L Na_2MoO_4, 0.12 g/L $NiCl_2$, 0.02 g/L $NaWO_4{\cdot}2H2O$, and 0.1 g/L Na_2SeO_4 was also added. Fumarate (40 mM) was used as an electron acceptor for growth of initial stocks picked from colonies, and acetate (20mM) was used as the sole electron and carbon source. Unless otherwise noted, the pH of the medium was adjusted to 6.8 and buffered with 2 g/L $NaHCO_3$, purged with N_2:CO_2 gas (80%/20%) passed over a heated copper column to remove trace oxygen, and autoclaved for 20 minutes at 121 degrees Celsius.

Here Table 1

X-ray diffraction (XRD) measurements: Approximately 0.2-0.5 g of untreated bulk mineral sample or 2.5 ml of mineral suspension in medium were analyzed by powder XRD. Minerals in basal media were separated from suspension by filtration (0.22 µm) in an anaerobic chamber (Coy Laboratory Products) under a N_2:CO_2:H_2 (75%:20%:5%) atmosphere, and stored in sealed mylar bags at -20 degrees Celsius prior to analysis. Diffractograms were measured from using 20° to 89° (2Θ) range, a step size of 0.02 2Θ, and a dwell of 0.5°/minute using a Rigaku MiniFlex ASC-6AM with a Co source. The resulting diffractograms were background subtracted, and phases were identified using Jade v9.1 software (MDI, Inc.).

Preparation of Fe(III)-(oxyhydr)oxides: "Poorly crystalline FeO(OH)" was produced after Lovley and Phillips, 1986, by adding 25% NaOH dropwise over 90 minutes to a rapidly stirring 0.4 M solution of $FeCl_3$ until the pH was 7.0. The solution was held at pH 7.0 for one hour, and the resulting suspension was washed with one volume of de-ionized and distilled water and used immediately (≤24 after synthesis) for XRD analysis and growth studies as rapid aging of such products to more crystalline minerals (e.g., goethite) has been observed even when kept in the dark at 4 degrees Celsius (Raven, Jain, & Loeppert, 1998). The untreated mineral was identified as akaganeite (β-FeOOH) by powder X-ray diffraction. Washing the mineral sample with up to three volumes of de-ionized and distilled water did not change the XRD pattern of the mineral or the reduction phenotypes observed.

Goethite and 2-line ferrihydrite (ca. $Fe_{10}O_{14}(OH)_2$) (Michel et al., 2007) were synthesized after Schwertmann and Cornell, 2000, with some modifications. For goethite, a solution of $FeCl_3$ was precipitated through neutralization with 5 N KOH, and the resulting alkaline mineral suspension was aged at 70 degrees Celsius for 60 hours to facilitate goethite formation. The suspension was then centrifuged, decanted, and washed with de-ionized and distilled water prior to freeze drying. For 2-line ferrihydrite, a solution of $FeCl_3$ was neutralized with KOH until the pH was 7.0. Suspensions were rinsed with de-ionized and distilled water and either freeze dried or centrifuged and suspended in a small volume of de-ionized and distilled water to concentrate the final product. Freeze dried samples yielded XRD patterns indicative of 2-line ferrihydrite, but suspension of hydrated samples in growth medium had an altered XRD pattern more similar to that of akaganeite. Freeze dried samples were stored at -80 degrees Celsius prior to addition to growth medium, while hydrated samples were used within 24 hours of synthesis.

Schwertmannite ($Fe_8O_8(OH)_6(SO_4)\cdot nH_2O$) was synthesized using a rapid precipitation method involving the addition of a 30% solution of H_2O_2 to a solution of $FeSO_4$ (Regenspurg, Brand, & Peiffer,

2004). The mixture was stirred rapidly for at least 12 hours until the pH was stable, at ~2.35. The solids were allowed to settle for 1 hour, and the supernatant carefully decanted. Solids were washed by centrifuging at 3,700 x g and suspending in 1 volume of de-ionized and distilled water. The product was concentrated by a final centrifugation at 3,700 x g for 5 minutes and resuspension in 1/20 the initial volume. XRD identified this initial product as schwertmannite, though subsequent addition to media at neutral pH values and autoclaving rapidly altered the mineral form.

Iron reduction assays: Basal media were prepared as above with some modifications. Fumarate was omitted as the Fe(III)-(oxyhydr)oxides were desired as the sole electron acceptor. NTA free trace mineral mix (in which all components were first dissolved in a small volume of HCl) was used in order to eliminate exogenous chelating compounds from the media. All media were purged with N_2:CO_2 gas (80%:20%) passed over a heated copper column to remove trace oxygen. Where indicated, media were autoclaved for 20 minutes at 121 degrees Celsius on a gravity cycle, and were immediately removed to cool at room temperature in the dark. As is standard for *G. sulfurreducens* medium containing Fe(III)-(oxyhydr)oxide (Caccavo et al., 1994), additional $NaH_2PO_4 \cdot H_2O$ (to a final concentration of 0.69 g/L) was added prior to autoclaving, as more recalcitrant and less reducible forms of Fe(III)-(oxyhydr)oxide will form when autoclaved without additional phosphate. For freshly precipitated akaganeite and 2-line ferrihydrite, 1 ml of the Fe-(oxyhydr)oxide suspension was added to 9 ml of basal medium. The final pH was adjusted by altering the pH of the basal medium prior to mineral addition and by altering the concentration of $NaHCO_3$ used prior to purging with anaerobic N_2:CO_2 gas (80%/20%). For goethite, an 88 g/L suspension was made in de-ionized and distilled water and 1 ml of this suspension was added to 9 ml of basal medium. The resulting medium had an effective Fe_{total} concentration of ~20 mM as determined by fully reducing an acidified sample with hydroxylamine and measuring the resulting Fe(II) using a modified Ferrozine assay (Lovley & Phillips, 1987). Because the synthesis of schwertmannite results in an acidic product below the pH at which *G. sulfurreducens* grows optimally (Caccavo et al.,

158 1994; Regenspurg et al., 2004), the mineral suspension was added to the basal medium (1:9) and the pH
159 of the solution was adjusted with NaOH and bicarbonate to produce a final pH of 6.8. For freeze dried 2-
160 line ferrihydrite, 0.2 grams of freeze dried sample was added per 10 ml of basal medium.

161 In all cases, 100 µl of electron acceptor-limited stationary phase cells (OD_{600} = 0.55) grown from
162 single colony picks in NB basal medium containing acetate (20 mM) and fumarate (40 mM) were used to
163 inoculate the Fe(III)-(oxyhydr)oxide containing media, with acetate provided as the electron and carbon
164 donor and the Fe(III)-(oxyhydr)oxide as the sole electron acceptor.

165 For all Fe(III)-(oxyhydr)oxide incubations except those involving goethite, a small sample was
166 removed at regular intervals and dissolved in 0.5 N HCl for at least 24 hours at 23-25 degrees Celsius in
167 the dark before the acid extractable Fe(II) present in the sample was measured. For incubations with
168 goethite, samples were incubated in 1 N HCl at 65 degrees Celsius for at least 24 hours in the dark,
169 followed by centrifugation at 13,000 x g for 10 minutes to remove solids. Fe(II) in the supernatant was
170 then measured.

171 **Manganese reduction assays:** Birnessite ($Na_xMn_{2-x}(IV)Mn(III)_xO_4$, x ~ 0.4) was prepared using the
172 protocol described in Chan, et al, 2015. Briefly, a solution of $KMnO_4$ was added to an equal volume of
173 $MnCl_2{\cdot}4H_2O$ solution and mixed vigorously. Solids were allowed to settle, and the overlaying liquid was
174 decanted off. The resulting solid was washed in de-ionized and distilled water and concentrated by
175 centrifugation. This suspension was added (~20mM) to basal medium containing acetate (10 mM) as the
176 carbon and electron donor. Cells were inoculated to a calculated OD_{600} of 0.005 from electron acceptor-
177 limited stationary phase cells. Mn(II) was measured indirectly as previously described (Chan et al., 2015;
178 Levar et al., 2014). Briefly, samples were acidified in 2 N HCl with 4 mM $FeSO_4$ added and allowed to
179 dissolve overnight at 25 degrees Celsius in the dark. After all solids were dissolved, the Fe(II)

concentration was measured. Because the reduction of Mn(IV) by Fe(II) is thermodynamically favorable, the measured Fe(II) concentration can be used to extrapolate the Mn(II) present a given sample.

Results:

The inner membrane multiheme cytochromes ImcH and CbcL are implicated in transfer of electrons out of the quinone pool when electron acceptors fall within different redox potential windows (Levar et al., 2014; Zacharoff et al., 2016). Mutants lacking *imcH* are only able to reduce poised electrodes with 'low' redox potentials (≤ -0.10 V vs. SHE), and are deficient in reduction of electrodes at redox potentials above this value (Levar et al., 2014). In contrast, *cbcL* mutants have the opposite phenotype, reducing electrodes with relatively high redox potentials, and having a deficiency in reduction of acceptors at or below -0.10 V vs. SHE (Zacharoff et al., 2016). These pathways are constitutive (Zacharoff et al., 2016), and use of each pathway appears to be able to switch in a matter of minutes during sweeps of increasing or decreasing potential known as catalytic cyclic voltammetry (Marsili, Rollefson, Baron, Hozalski, & Bond, 2008; Yoho, Popat, & Torres, 2014; Zacharoff et al., 2016).

A simple experiment testing if these two pathways could also be essential for reduction of 'low' and 'high' potential metal oxide acceptors is shown in Figure 1. When wild type *G. sulfurreducens* was compared to markerless deletion mutants lacking each pathway, mutants lacking ImcH could not reduce laboratory synthesized birnessite (a ~+0.35 V acceptor), while CbcL mutants could not reduce goethite (a ~-0.17 V acceptor) (Majzlan, 2012; Nealson & Myers, 1992; Orsetti, Laskov, & Haderlein, 2013; Thamdrup, 2000; Thauer et al., 1977) (Figure 1). These observations were consistent with redox potential preferences first described with electrodes poised at +0.24 or -0.10 V vs. SHE, and show the utility of using these strains to report the effective redox potentials of minerals (Chan et al., 2015; Levar et al., 2014; Zacharoff et al., 2016).

Here Figure 1

Evidence that the electron transfer pathway changes even in the absence of XRD-pattern changes

Most Fe(III)-(oxyhydr)oxides do not exist at these high or low extremes, but possess electron accepting potentials predicted to lie near the -0.10 V redox potential threshold that requires a transition from ImcH-dependent to the CbcL-dependent reduction pathways in electrode-grown cells (Levar et al., 2014; Majzlan et al., 2004; Majzlan, 2012; Thamdrup, 2000; Zacharoff et al., 2016). While testing this with electrodes is straightforward, the redox potential of Fe(III)-(oxyhydr)oxides in this range is not easy to predict or measure (Sander et al., 2015). Aging (accelerated by autoclaving or freeze drying) can increase particle size and lower redox potential, or drive re-crystallization to lower redox potential forms (Navrotsky et al., 2008; Roden, Urrutia, & Mann, 2000; Roden & Zachara, 1996; Roden, 2006; Thamdrup, 2000). As Fe(III)-(oxyhydr)oxide reduction is a proton consuming reaction (Kostka & Nealson, 1995; Majzlan, 2012; Thamdrup, 2000), for each unit decrease in pH, the redox potential of the Fe(III)/Fe(II) redox couple increases by ~59 mV per the Nernst equation (Bonneville, Van Cappellen, & Behrends, 2004; Kostka & Nealson, 1995; Majzlan, 2012; Thamdrup, 2000).

To test the hypothesis that *G. sulfurreducens* also utilizes ImcH- or CbcL-dependent pathways to reduce minerals on the basis of redox potential, we prepared Fe(III)-(oxyhydr)oxides by slow precipitation of $FeCl_3$ with NaOH (Lovley & Phillips, 1986), and characterized minerals before and after addition to medium using XRD. While Fe(III)-(oxyhydr)oxides prepared in this manner are often referred to as “poorly crystalline” or “amorphous”, all XRD signatures of our preparations were consistent with akaganite (β-FeOOH) (Figure 2E). Because the β-FeOOH/Fe(II) redox couple has a midpoint potential near -0.10 V vs. SHE (Majzlan, 2012), a fresh, fully oxidized suspension of fresh akaganeite would initially have a redox potential above 0 V vs SHE, and theoretically require only the ‘high’ potential pathway of *G. sulfurreducens*.

When wild-type, Δ*imcH,* and Δ*cbcL* strains were incubated with freshly precipitated akaganeite, wild-type cultures rapidly reduced the provided Fe(III)-(oxyhydr)oxide. The Δ*cbcL* cultures containing the high-potential pathway initially reduced fresh akaganeite at rates similar to wild type, but reduction slowed as Fe(II) accumulated, and the concentration of Fe(II) never reached the extent of wild type. In contrast, Δ*imcH* cultures lacking the high potential pathway demonstrated a substantial lag, remaining near background for 7 days (Figure 2A). Once metal reduction began, Δ*imcH* cultures were able to reach the final extent observed in wild type. No reduction was observed in cell-free controls.

When medium containing akaganeite was autoclaved to lower redox potential due to accelerated aging, both wild type and Δ*cbcL* performed similarly, but the lag observed with Δ*imcH* was much shorter (Figure 2B). Despite the substantial change in the Δ*imcH* Fe(III)-(oxyhydr)oxide reduction phenotype, the XRD pattern before and after autoclaving was similar (Figure 2E). Such a lack of XRD alteration in response to autoclaving has been previously noted (Hansel et al., 2015). This suggests that phenotypic changes were due to mineral alteration outcomes not detected by powder XRD, such as short-range structural order or particle aggregation, that lowered effective redox potential and allowed growth of the Δ*imcH* strain lacking the high-potential pathway.

Reduction phenotypes also respond to changes in medium pH that alter redox potential

The lag in extracellular electron transfer by Δ*imcH*, in contrast to immediate reduction by Δ*cbcL,* suggests that fresh akaganeite has an initial redox potential greater than -0.10 V vs. SHE. Based on this hypothesis, only after a small amount of Fe(II) accumulates does potential drop into a range reducible by Δ*imcH*. Similarly, aging fresh akaganite by autoclaving shortened the lag in Figure 2B likely by lowering redox potential. If this is true, then manipulations designed to raise redox potential should extend this lag or prevent Δ*imcH* from reducing akaganeite altogether.

Because Fe(III)-(oxyhydr)oxide reduction is a proton consuming reaction, decreasing pH will increase the redox potential, an effect that has been used to explain magnetite reduction by *Shewanella oneidensis* (Kostka & Nealson, 1995; Majzlan, 2012; Thamdrup, 2000). When the pH of basal medium containing akaganeite was adjusted to 6.3 (raising the redox potential ~30 mV), near complete inhibition of reduction by Δ*imcH* was observed (Figure 2C). Autoclaving pH 6.3 akaganeite medium was not sufficient to restore the reduction phenotype of Δ*imcH*, but did aid reduction by Δ*cbcL* (Figure 2D). As with medium at pH 6.8, autoclaving at 6.3 did not substantially alter the XRD pattern of the mineral provided (Figure 2E). Importantly, wild type, Δ*imcH,* and Δ*cbcL* grew without significant defects at pH values of 6.3 or 6.8 in control experiments containing fumarate as the sole terminal electron acceptor (Table 1). Based on these results, when akaganeite is autoclaved at pH 6.8, the initial redox potential is lowered close to -0.10 V vs. SHE, permitting wild-type extents of reduction by cells containing the CbcL-dependent, low-potential pathway. Fresh akaganeite, especially at pH 6.3, behaves consistent with a redox potential of 0 V or greater, thus preventing reduction by cells containing only the low-potential pathway.

Here Figure 2

These two experiments, using aging to reduce redox potential and pH to raise redox potential, caused changes in Δ*imcH* phenotypes that provided evidence that *G. sulfurreducens* discriminates between extracellular electron acceptors independent of the mineral properties accessed by powder XRD. They also pointed to best practices for medium preparation in order to obtain consistent results if the question involves the *initial* redox conditions created by a mineral, and the proteins needed for electron transfer under those *initial* conditions. The amount of Fe(II) accumulated after 7 days provided a repeatable readout of the ability of a *G. sulfurreducens* strain or mutant reduce a given Fe(III)-

(oxyhydr)oxide. According to this assay, the more Fe(II) produced in 7 days by an Δ*imcH* mutant, the lower the initial redox potential of the mineral.

Other mineral forms consistent with a multiple-pathway model

A variety of Fe(III)-(oxyhydr)oxide minerals were then synthesized to test interactions of these variables. When schwertmannite was synthesized using a rapid precipitation method (Regenspurg et al., 2004), the mineral was stable at pH values below pH 4.0 and its structure could be confirmed by XRD. However, abiotic transformation of schwertmannite to other mineral forms is accelerated at pH values greater than 4.5 (Blodau & Knorr, 2006) and analysis of XRD patterns after schwertmannite was added to *Geobacter* growth medium revealed rapid formation of XRD-amorphous minerals (Figure 3E). Reduction phenotypes suggested this fresh mineral also produced a redox potential near 0 V vs. SHE, as cells lacking the high potential pathway (Δ*imcH*) showed a lag at pH 6.8, which was shorter after the mineral was autoclaved (Figure 3B). Reduction by Δ*imcH* was worst when the redox potential was further raised by buffering to pH 6.3 (Figure 3C), while autoclaving pH 6.3 medium allowed a small amount of Fe(II) accumulation that ended the lag after >8 days.

Here Figure 3

When Fe(III)-(oxyhrdr)oxide was prepared according to the 2-line ferrihydrite protocol of Schwertmann and Cornell (2000), patterns were again similar to those observed with akaganite and schwertmannite. Freshly prepared mineral was reduced by Δ*cbcL* to within 67% of wild type after seven days. When this mineral was freeze dried (resulting in XRD-confirmed 2-line ferrihydrite), reduction by Δ*cbcL* was less than 30% of wild type, suggesting that freeze drying lowered redox potential of the mineral to a point where the low-potential pathway, encoded by *cbcL,* was more important. Changing pH by 0.5 units was not sufficient to alter reduction phenotypes, consistent with the freeze drying process lowering redox potential of ferrihydrite much more than 30 mV of pH change could overcome.

293 A general trend emerged during these experiments, consistent with autoclaving, freeze drying,
294 and pH influencing redox potential in similar ways, regardless of the mineral. When reduction by Δ*imcH*
295 was near wild-type levels, reduction by Δ*cbcL* was typically at its lowest. When reduction by Δ*cbcL* was
296 near wild-type levels, Δ*imcH* cultures failed to reduce the provided electron acceptor. Figure 4
297 represents all seven-day reduction data from 17 different XRD-characterized mineral forms incubated
298 with three different strains, ranked according to Δ*imcH* performance. This trend suggests the two
299 mutants act as an *in vivo* sensor of initial redox potential, across a suite of minerals and conditions.

300 For example, if initial conditions were well above 0 V vs. SHE, such as with freshly precipitated
301 minerals in medium at pH 6.3, Δ*imcH* mutants lacking the high potential pathway were unable to
302 respire. When exposed to the same minerals, Δ*cbcL* mutants containing only the high potential pathway
303 performed similar to wild type. As minerals were aged or manipulated to lower their initial redox
304 potential, the CbcL-dependent pathway became increasingly important to achieve wild-type extents of
305 reduction. These incubations highlighted the different contributions of ImcH and CbcL to the initial rate
306 vs. final extent of Fe(III) reduction, respectively.

307 Interestingly, some level of metal reduction was always observed for Δ*cbcL* mutants exposed to
308 minerals predicted to be very low potential acceptors. This result is similar to previous studies where
309 Δ*cbcL* still demonstrated a slow but detectable rate of respiration on electrodes poised at low redox
310 potentials (Zacharoff et al., 2016). This activity may reflect a yet-undiscovered pathway used under
311 thermodynamically challenging conditions, where neither ImcH- nor CbcL-dependent pathways can
312 function.

313 The results in Figure 4 represent a suite of minerals (2-line ferrihydrite, goethite, akaganeite,
314 schwertmannite, and birnessite), in which additional variability is introduced through freeze-drying,
315 autoclaving, and pH adjustments. These variables could alter mineral crystal structure, particle size,

316 degree of aggregation, surface area, and surface charge, and thus influence microbial attachment or
317 behavior in unpredictable ways (Cutting, et al., 2009; Majzlan et al., 2004; Navrotsky et al., 2008; Roden,
318 2006). However, all of these manipulations change redox potential in predictable ways. Further, these
319 phenotypes are caused by the deletion of genes encoding inner membrane proteins, far from the outer
320 surface reduction step(s) where metal charge or structure should play an important role. Based on the
321 overall pattern of responses, we propose that redox potential should be viewed as a master variable
322 affecting the pathway of extracellular electron acceptor reduction used by *G. sulfurreducens*.

323 **Here Figure 4**

324 **Cells lacking the CbcL-dependent pathway have increased growth yield.**

325 A key question stemming from this work relates to the evolutionary forces selecting for multiple
326 electron transfer pathways at the inner membrane. As Δ*imcH* cells are often able to completely reduce a
327 provided mineral after a small amount of Fe(II) accumulates, why not encode a single, CbcL-dependent
328 electron transfer pathway and allow it operate at all potentials? One hypothesis is that *G. sulfurreducens*
329 is able to take advantage of the different amounts of energy represented by different metal
330 (oxyhydr)oxides.

331 To test this hypothesis, the cell yield of *G. sulfurreducens* strains in which one pathway was
332 removed was measured. Because both Δ*imcH* and Δ*cbcL* can initially reduce akaganeite (albeit to
333 different extents), direct comparisons were possible when a low inoculum of each strain was added to
334 medium containing this mineral (autoclaved at pH 6.8, as in Figure 2B) and incubated. Samples were
335 removed for measurement of Fe(II) and direct plate counts on solid minimal medium. In all experiments,
336 Δ*cbcL* generated more colony forming units per mol Fe(II) produced than either wild type *G.*
337 *sulfurreducens* or Δ*imcH*. For each mM of Fe(III) reduced, Δ*cbcL* produced 2.5 ± 0.3 x 10^6 CFU, while wild
338 type and Δ*imcH* produced 0.8 ± 0.1 and 1.6 ± 0.1 x 10^6 CFU, respectively (n=5 for each strain). These

results indicated that when electron flow was forced through the ImcH-dependent pathway (as in Δ*cbcL*), more cells were produced per Fe(III) reduced.

Cell attachment to mineral particles could confound plate counts in experiments with cells grown on solid particles. When wild type *G. sulfurreducens* CFU were measured over the course of akaganeite reduction, a decrease was seen for time points shortly after inoculation when Fe(II) begins to rapidly accumulate, which may suggest an association of cells to akaganeite particles or aggregation of cells to other cells. In a second series of experiments, basal medium containing acetate and fumarate was inoculated with a 2 % v/v inoculum from akaganeite-grown cultures. Because all wild-type and mutant cultures grow at similar rates with fumarate as the electron acceptor (see Table 1), the point at which optical density is detectable in fumarate grown cultures is a function of the number of cells in the initial inoculum. In all of these experiments, Δ*cbcL* again demonstrated significantly more cells per mol Fe(II) than did wild type or Δ*imcH.*

These fumarate outgrowth experiments, which reflect the total number of cells in the mineral containing medium at a given time point, agreed with the trend seen in direct plate counts from akaganeite cultures. In both cases, Δ*cbcL* generated more cells per mol Fe(III) reduced than either wild type or Δ*imcH*. When normalized to the amount of Fe(II) produced, Δ*cbcL* yield was 246.2% ± 15.11 of that of wild-type, whereas Δ*imcH* yield was 105.2% ± 24.33 (n=3 in both cases). Combined with previous data showing that the ImcH-dependent pathways support faster growth rates when electrodes poised at +0.24 V vs. SHE (Zacharoff et al., 2016), this supports the hypothesis that *G. sulfurreducens* alters its electron transfer pathway to use a higher yield pathway whenever possible. Somehow, these inner membrane pathways are able to switch 'on' and 'off' in response to the redox potential of external electron acceptors. This difference provides one explanation for maintaining the complexity and burden associated with encoding multiple pathways of electron transfer across the inner membrane.

Discussion:

Fe(III)-(oxyhydr)oxide minerals in nature exist as a complex continuum of potential energies. As such, it is unsurprising that bacteria would evolve equally complex mechanisms able to harness the energy available during respiration to these metals. While a single pathway essential for reduction of all metals emerged in the model metal-reducing *Shewanella spp.,* a similarly simple solution has remained elusive in *Geobacter spp.*. The data reported here demonstrates that even under the most common laboratory conditions where Fe(III)-(oxyhydr)oxide is precipitated and added to medium, *G. sulfurreducens* will utilize multiple electron transfer pathways to accomplish what is considered to be wild-type levels of Fe(III) reduction. For Fe(III)-(oxyhydr)oxides that are predicted to have redox potentials around 0 V, such as schwertmannite, akaganeite, and ferrihydrite, the electron-accepting potential decreases as Fe(II) accumulates, and triggers utilization of electron transfer pathways that support lower cell yield and slower growth rate, but still allow some respiration. The ability of *G. sulfurreducens* to respond to the changing redox potential of its environment likely allows this organism to make the most efficient use of the provided mineral.

Based on proteomic studies, *G. sulfurreducens* expresses at least 78 expressed multiheme *c*-type cytochromes, yet mutant analyses were initially unable to link particular cytochromes to reduction of specific extracellular electron acceptors (Aklujkar et al., 2013; Leang et al., 2003, 2010; Rollefson et al., 2009, 2011; Shi et al., 2007). One possible source of cytochrome diversity could be separate pathways required for soluble Fe(III)-citrate, insoluble Fe(III)-(oxyhydr)oxides, and Mn(IV)-(oxyhydr)oxides. However, despite their many differences, Fe(III)-citrate and Mn(IV)-(oxyhydr)oxides both represent high potential acceptors, from the viewpoint of the inner membrane. As we detect evidence for at least one other pathway in this work, and the *G. sulfurreducens* genome appears to encode at least 4 other inner membrane quinone oxidoreductases, redox potential differences may help to explain additional cytochrome complexity of *Geobacter.* Possessing protein machinery able extract the full advantage from

386 minerals as they descend through the redox tower also helps explain the dominance of these metal-
387 reducing organisms in contaminated subsurface environments undergoing rapid redox potential
388 changes.

389 In order to characterize and biochemically dissect extracellular electron transfer in dissimilatory
390 metal reducing organisms such as *G. sulfurreducens*, closer attention may need to be paid not just to
391 crystal structure, but the actual redox potential experienced by the organisms interacting with these
392 minerals. Commonly synthesized Fe-(oxyhydr)oxides prepared by precipitation of Fe(III) can produce
393 very different rates of reduction or mutant phenotypes depending on the age of the material and the
394 length of time one is willing to incubate cells. A distinction between initial rates of Fe(III)-(oxyhydr)oxide
395 reduction, where higher-potential conditions exist, and final extent of reduction achieved by lower
396 potential pathways may help separate some of these confounding effects. One would also expect
397 significant differences in washed cell suspensions, where the degree of respiratory coupling to growth is
398 not part of the assay, since electron flow through the ImcH- and CbcL-dependent pathways support
399 different growth rates and yields.

400 It now appears that in *G. sulfurreducens* a transition from an ImcH-dependent electron transfer
401 pathway to a CbcL-dependent pathway occurs both when electrodes and many commonly used Fe(III)-
402 (oxyhydr)oxides are provided as sole terminal electron acceptors. The initial rate and total extent of
403 Fe(III)-(oxyhydr)oxide reduction may also be the result of a series of redox potential dependent
404 processes in environmental samples, with each step supporting different cell yields. Competition in the
405 environment could occur along any part of this continuum, rewarding those capable of rapid growth
406 when the Fe(III)-(oxyhydr)oxide is high potential, or those able to survive with electron acceptors at
407 relatively low redox potentials. The prevalence of ImcH and CbcL homologues in other dissimilatory
408 metal reducing organisms and in metagenomics data from sites undergoing active metal reduction

409 (Levar et al., 2014; Zacharoff et al., 2016) suggests that this type of redox discrimination may also occur
410 in diverse organisms, and provides interesting opportunities for further exploration of redox potential
411 dependent respiration in these organisms and environments.

412

413 **References:**

414 Aklujkar, M. A., Coppi, M. V, Leang, C., Kim, B. C., Chavan, M. A., Perpetua, L. A., … Holmes, D. E. (2013).
415 Proteins involved in electron transfer to Fe(III) and Mn(IV) oxides by Geobacter sulfurreducens and
416 Geobacter uraniireducens. *Microbiology*, *159*, 515–535.

417 Blodau, C., & Knorr, K. H. (2006). Experimental inflow of groundwater induces a "biogeochemical regime
418 shift" in iron-rich and acidic sediments. *Journal of Geophysical Research: Biogeosciences*, *111*, 1–
419 12.

420 Bonneville, S., Van Cappellen, P., & Behrends, T. (2004). Microbial reduction of iron(III) oxyhydroxides:
421 Effects of mineral solubility and availability. *Chemical Geology*, *212*, 255–268.

422 Caccavo, F., Lonergan, D. J., Lovley, D. R., Davis, M., Stolz, J. F., & McInerney, M. J. (1994). *Geobacter*
423 *sulfurreducens sp. nov.*, a hydrogen- and acetate-oxidizing dissimilatory metal-reducing
424 microorganism. *Applied and Environmental Microbiology*, *60*, 3752–3759.

425 Chan, C. H., Levar, C. E., Zacharoff, L., Badalamenti, J. P., & Bond, D. R. (2015). Scarless genome editing
426 and stable inducible expression vectors for *Geobacter sulfurreducens*. *Applied and Environmental*
427 *Microbiology*, *81*, 7178-7186.

428 Cutting, R. S., Coker, V. S., Fellowes, J. W., Lloyd, J. R., & Vaughan, D. J. (2009). Mineralogical and
429 morphological constraints on the reduction of Fe(III) minerals by *Geobacter sulfurreducens*.
430 *Geochimica et Cosmochimica Acta*, *73*, 4004–4022.

431 Green, J., & Paget, M. S. (2004). Bacterial redox sensors. *Nature Reviews Microbiology*, *2*, 954–966.

432 Hansel, C. M., Lentini, C. J., Tang, Y., Johnston, D. T., Wankel, S. D., & Jardine, P. M. (2015). Dominance of
433 sulfur-fueled iron oxide reduction in low-sulfate freshwater sediments. *The ISME Journal*, *9*, 2400-
434 2412.

435 Kostka, J. E., & Nealson, K. H. (1995). Dissolution and reduction of magnetite by bacteria. *Environmental*
436 *Science & Technology*, *29*, 2535–2540.

437 Leang, C., Coppi, M. V, & Lovley, D. R. (2003). OmcB, a *c*-type polyheme cytochrome, involved in Fe(III)
438 reduction in *Geobacter sulfurreducens*. *Journal of Bacteriology*, *185*, 2096–2103.

439 Leang, C., Qian, X., Mester, T., & Lovley, D. R. (2010). Alignment of the *c*-type cytochrome OmcS along
440 pili of *Geobacter sulfurreducens*. *Applied and Environmental Microbiology*, *76*, 4080–4084.

441 Levar, C. E., Chan, C. H., Mehta-Kolte, M. G., & Bond, D. R. (2014). An inner membrane cytochrome
442 required only for reduction of high redox potential extracellular electron acceptors. *MBio*, *5*,
443 e02034.

444 Lovley, D. R., & Phillips, E. J. (1986). Organic matter mineralization with reduction of ferric iron in
445 anaerobic sediments. *Applied and Environmental Microbiology*, *51*, 683–689.

446 Lovley, D. R., & Phillips, E. J. (1987). Rapid assay for microbially reducible ferric iron in aquatic sediments.
447 *Applied and Environmental Microbiology*, *53*, 1536–1540.

448 Majzlan, J. (2011). Thermodynamic stabilization of hydrous ferric oxide by adsorption of phosphate and
449 arsenate. *Environmental Science & Technology*, *45*, 4726–4732.

450 Majzlan, J. (2012). Minerals and Aqueous Species of Iron and Manganese as Reactants and Products of
451 Microbial Metal Respiration. In J. Gescher & A. Kappler (Eds.), *Microbial Metal Respiration; From*
452 *Geochemistry to Potential Applications* (1st ed., pp. 1–28). Springer.

453 Majzlan, J., Navrotsky, A., & Schwertmann, U. (2004). Thermodynamics of iron oxides: Part III. Enthalpies
454 of formation and stability of ferrihydrite (~$Fe(OH)_3$), schwertmannite (~$FeO(OH)_{3/4}(SO_4)_{1/8}$), and ε-
455 Fe_2O_3. *Geochimica et Cosmochimica Acta*, *68*, 1049–1059.

456 Marsili, E., Rollefson, J. B., Baron, D. B., Hozalski, R. M., & Bond, D. R. (2008). Microbial biofilm
457 voltammetry: direct electrochemical characterization of catalytic electrode-attached biofilms.
458 *Applied and Environmental Microbiology*, *74*, 7329–7337.

459 Michel, F. M., Ehm, L., Antao, S. M., Lee, P. L., Chupas, P. J., Liu, G., … Parise, J. B. (2007). The structure of
460 ferrihydrite, a nanocrystalline material. *Science*, *316*, 1726–1729.

461 Navrotsky, A., Mazeina, L., & Majzlan, J. (2008). Size-driven structural and thermodynamic complexity in
462 iron oxides. *Science*, *319*, 1635–1638.

463 Nealson, K. H., & Myers, C. R. (1992). Microbial reduction of manganese and iron: New approaches to
464 carbon cycling. *Applied and Environmental Microbiology*, *58*, 439–443.

465 Nealson, K. H., & Saffarini, D. (1994). Iron and manganese in anaerobic respiration: environmental
466 significance, physiology, and regulation. *Annual Review of Microbiology*, *48*, 311-343.

467 Orsetti, S., Laskov, C., & Haderlein, S. B. (2013). Electron transfer between iron minerals and quinones:
468 estimating the reduction potential of the Fe(II)-goethite surface from AQDS speciation.
469 *Environmental Science & Technology*, *47*, 14161–14168.

470 Post, J. E., & Veblen, D. R. (1990). Crystal structure determinations of synthetic sodium, magnesium, and
471 potassium birnessite using TEM and the Rietveld method. *American Mineralogist*, *75*, 477–489.

472 Raven, K. P., Jain, A., & Loeppert, R. H. (1998). Arsenite and arsenate adsorption on ferrihydrite: Kinetics,
473 equilibrium, and adsorption envelopes. *Environmental Science and Technology*, *32*, 344–349.

474 Regenspurg, S., Brand, A., & Peiffer, S. (2004). Formation and stability of schwertmannite in acidic
475 mining lakes. *Geochimica et Cosmochimica Acta*, *68*, 1185–1197.

476 Roden, E. E. (2006). Geochemical and microbiological controls on dissimilatory iron reduction. *Comptes*
477 *Rendus Geoscience*, *338*(, 456–467.

478 Roden, E. E., Urrutia, M. M., & Mann, C. J. (2000). Bacterial reductive dissolution of crystalline Fe (III)
479 oxide in continuous-flow column reactors. *Applied and Environmental Microbiology, 66*, 1062–
480 1065.

481 Roden, E. E., & Zachara, J. M. (1996). Microbial reduction of crystalline iron(III) oxides: Influence of oxide
482 surface area and potential for cell growth. *Environmental Science & Technology*, *30*, 1618–1628.

483 Rollefson, J. B., Levar, C. E., & Bond, D. R. (2009). Identification of genes involved in biofilm formation
484 and respiration via mini-*Himar* transposon mutagenesis of *Geobacter sulfurreducens*. *Journal of*
485 *Bacteriology*, *191*, 4207–4217.

486 Rollefson, J. B., Stephen, C. S., Tien, M., & Bond, D. R. (2011). Identification of an extracellular
487 polysaccharide network essential for cytochrome anchoring and biofilm formation in *Geobacter*
488 *sulfurreducens*. *Journal of Bacteriology*, *193*, 1023–1033.

489 Russell, J. B., & Cook, G. M. (1995). Energetics of bacterial growth: balance of anabolic and catabolic
490 reactions. *Microbiological Reviews*, *59*(1), 48–62.

491 Sander, M., Hofstetter, T. B., & Gorski, C. A. (2015). Electrochemical analyses of redox-active iron
492 minerals: A review of non-mediated and mediated approaches. *Environmental Science &*
493 *Technology*, *49,* 5862-5878.

494 Schwertmann, U., & Cornell, R. M. (2000). *Iron Oxides in the Laboratory: Preparation and*
495 *Characterization* (2nd ed.). Wiley-VCH.

496 Shi, L., Squier, T. C., Zachara, J. M., & Fredrickson, J. K. (2007). Respiration of metal (hydr)oxides by
497 *Shewanella* and *Geobacter*: a key role for multihaem *c*-type cytochromes. *Molecular Microbiology*,
498 *65*, 12–20.

499 Thamdrup, B. (2000). Bacterial manganese and iron reduction in aquatic sediments. In B. Schink (Ed.),
500 *Advances in Microbial Ecology* (16th ed., pp. 41–84). Springer.

501 Thauer, R. K., Jungermann, K., Decker, K., & Pi, P. P. H. (1977). Energy conservation in chemotrophic
502 anaerobic bacteria. *Bacteriological Reviews*, *41*, 100-180.

503 Yoho, R. A., Popat, S. C., & Torres, C. I. (2014). Dynamic potential-dependent electron transport pathway
504 shifts in anode biofilms of *Geobacter sulfurreducens*. *ChemSusChem*, *7*, 3413-3419.

505 Zacharoff, L., Chan, C. H., & Bond, D. R. (2016). Reduction of low potential electron acceptors requires
506 the CbcL inner membrane cytochrome of *Geobacter sulfurreducens*. *Bioelectrochemistry*, *107*, 7-13.

Table 1

Strain	Source	Doubling time in minimal medium at different pH (hours)*	
		6.3	6.8
Geobacter sulfurreducens			
Wild type (ATCC 51573)	Caccavo et al., 1994	6.5±0.2	5.6±0.2
Δ*cbcL*	Zacharoff et al., 2016	5.6±0.2	6.4±0.1
Δ*imcH*	Chi Ho Chan et al., 2015	5.7±0.1	6.0±0.2

* Doubling times are the mean and standard deviation of at least two idependent experiments of triplicate cultures

Figure 1

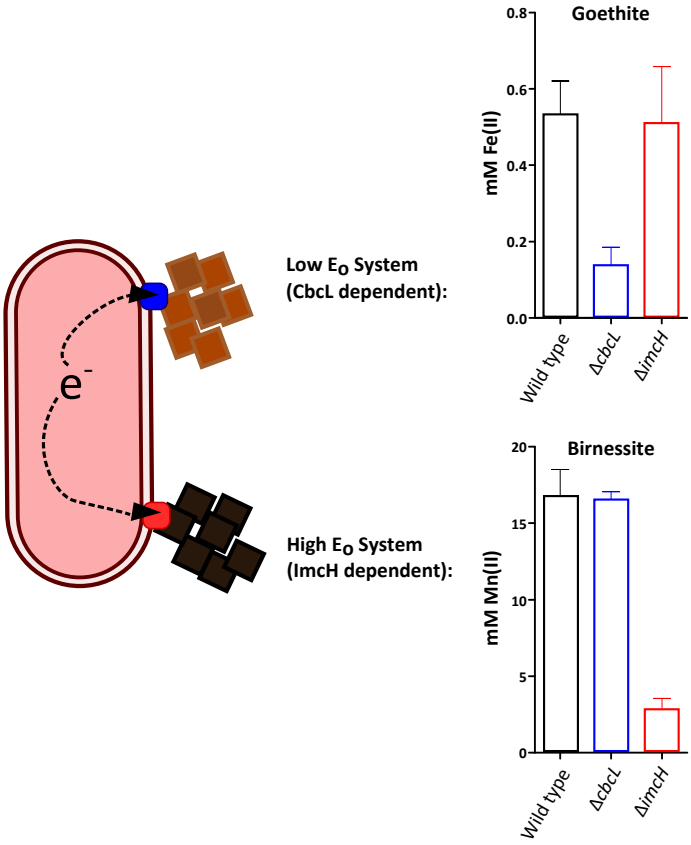

G. sulfurreducens *requires at least two distinct electron transfer pathways for the reduction of minerals*: Wild type *G. sulfurreducens* has the ability to reduce extracellular electron acceptors ranging from the low potential Fe(III)-(oxyhydr)oxide goethite (α-FeOOH) to the high potential Mn(IV)-oxide birnessite ($Na_xMn_{2-x}(IV)Mn(III)_xO_4$, x ~ 0.4). Mutants deficient in CbcL or ImcH show reduction phenotypes consistent with redox potential discrimination. Δ*cbcL* reduces birnessite as well as wild type, but fails to reduce goethite after 14 days of incubation. Δ*imcH* reduces goethite as well as wild type, but is unable to reduce birnessite. Data shown are the mean and standard deviation of triplicate cultures.

Figure 2

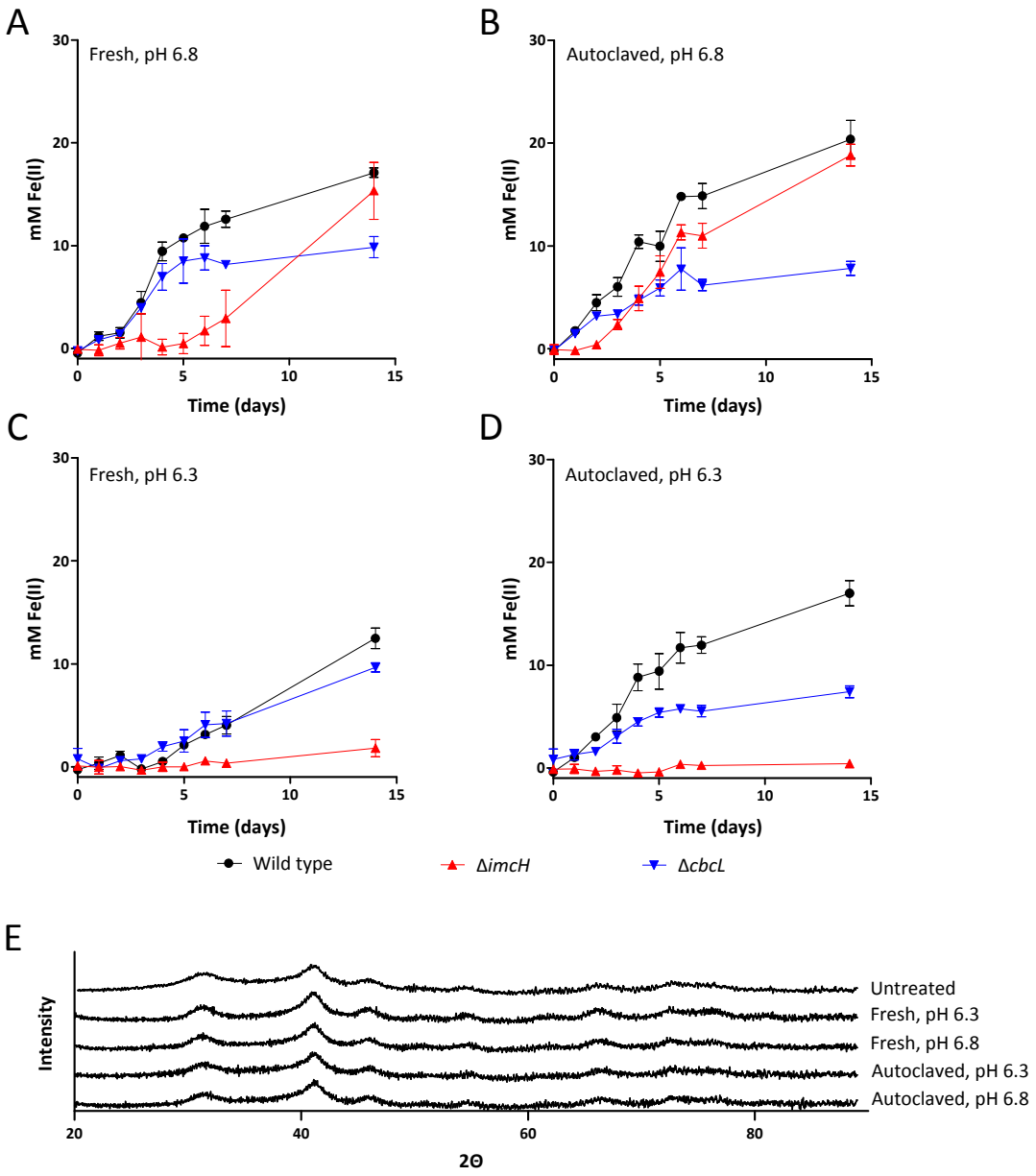

Autoclaving and changing pH alters mutant phenotypes. In all cases, wild type is represented by black circles, Δ*cbcL* by downward pointing blue triangles, and Δ*imcH* by upward pointing red triangles. (A) A long lag is observed for Δ*imcH* inoculated into medium with no autoclaving. (B) The lag observed for Δ*imcH* is decreased when the medium is aged through autoclaving. (C) Decreasing the pH by 0.5 units eliminates akaganeite reduction by Δ*imcH*. (D). Aging pH 6.3 medium through autoclaving is not sufficient to decrease the redox potential enough to allow for reduction by Δ*imcH*. All data shown are the mean and standard deviation for triplicate cultures, and are representative of at least duplicate incubations. (E) XRD patterns of the mineral used in panels A-D. The XRD pattern for the freshly precipitated mineral is also shown. No changes in XRD patterns were observed between multiple batches of synthesis and media preparation, suggesting that differences in Δ*imcH* behavior are due to changes in the initial redox potential of the medium.

Figure 3

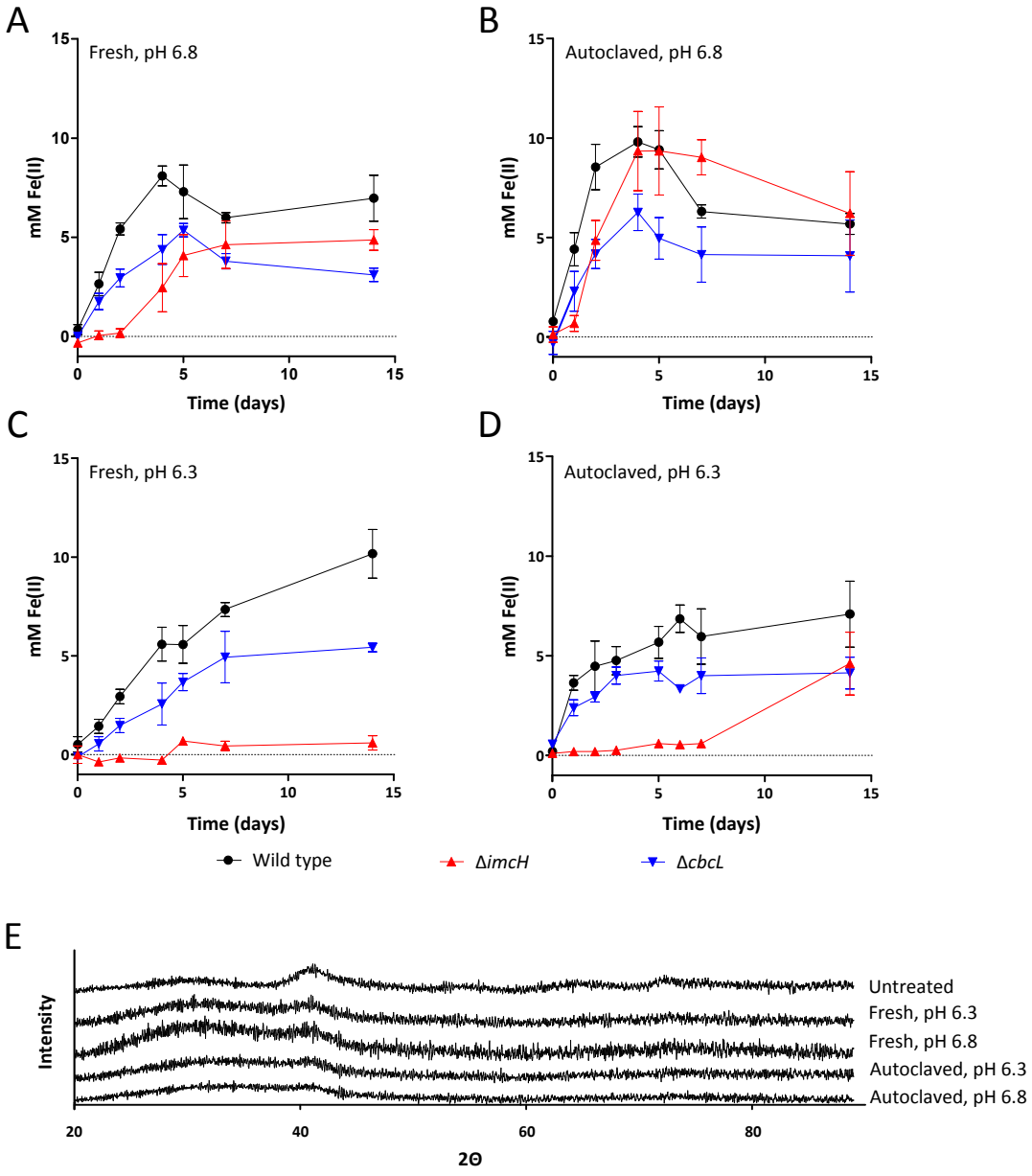

Treatment of schwertmannite with growth medium at pH 6.3 or pH 6.8 alters mineralogy: Rapid precipitation of an Fe sulfide solution with hydrogen peroxide yields XRD-pure schwertmannite ("untreated", Panel E), but when this mineral suspension is added to growth medium and adjusted to circumneutral pH values, abiotic transformation to other mineral forms is observed. Autoclaving these media lead to further mineral transformation.

Figure 4

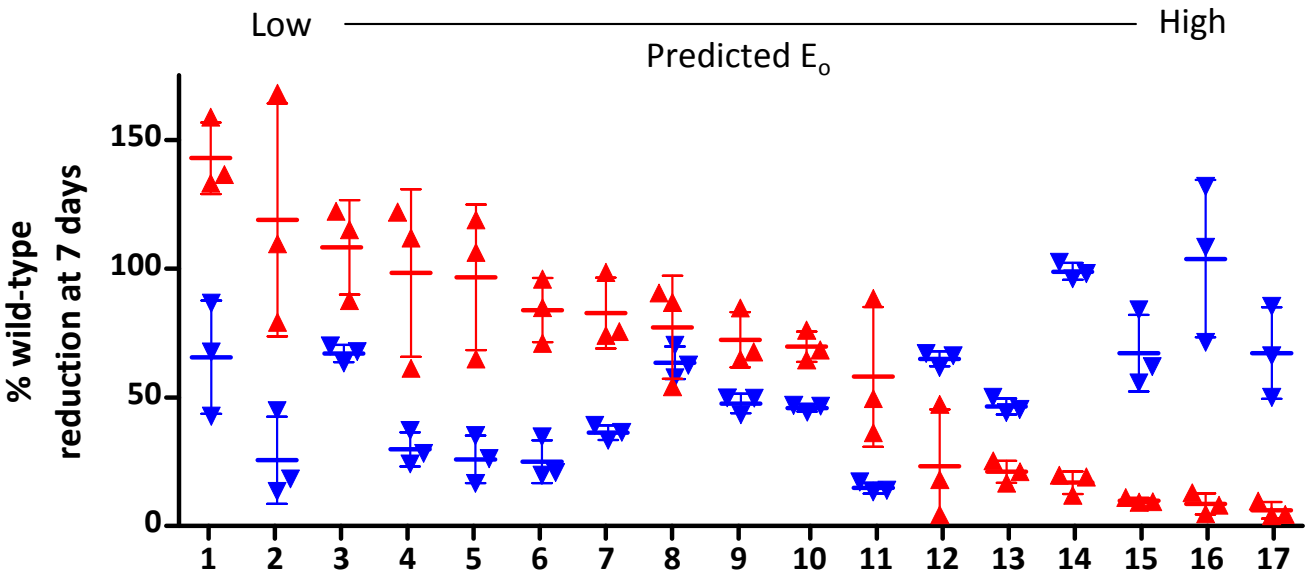

#	Starting mineral*	Freeze dried (Y/N)	Autoclaved (Y/N)	pH	Resulting mineral†
1	Schwertmannite	N	Y	6.8	XRD Amorphous
2	2-line Fh	Y	N	6.3	2-line Fh
3	2-line Fh	N	N	6.8	Akaganeite
4	Goethite	Y	N	6.8	Goethite
5	2-line Fh	Y	N	6.8	2-line Fh
6	2-line Fh	Y	Y	6.3	2-line Fh
7	Akaganeite	N	Y	6.8	Akaganeite
8	Schwertmannite	N	N	6.8	XRD Amorphous
9	Akaganeite	N	Y	6.6	Akaganeite
10	Akaganeite	N	Y	6.5	Akaganeite
11	2-line Fh	Y	Y	6.8	2-line Fh
12	Akaganeite	N	N	6.8	Akaganeite
13	Akaganeite	N	Y	6.3	Akaganeite
14	Birnessite	N	N	6.8	Birnessite
15	Schwertmannite	N	Y	6.3	XRD Amorphous
16	Akaganeite	N	N	6.3	Akaganeite
17	Schwertmannite	N	N	6.3	XRD Amorphous

*Listed mineral is mineral identity prior to treatment with media or autoclaving.

†Listed mineral is mineral identity after treatmeant with media or autoclaving and before innoculation with *G. sulfurreducens*

G. sulfurreducens *requires both ImcH and CbcL for complete reduction of a range of minerals:* Cultures of Δ*imcH* (red upward pointing triangles) and Δ*cbcL* (blue downward pointing triangles) were incubated with minerals as the sole terminal electron acceptor, and the extent of Fe(II) or Mn(II) accumulation after seven days of incubation were measured relative to that of wild type *G. sulfurreducens*. Conditions are ordered left to right in order of Δ*imcH* reduction, from best to worst. Akaganeite, β-FeOOH. Schwertmannite, $Fe_8O_8(OH)_6(SO_4)\cdot nH_2O$. 2-line Fh (Ferrihydrite), ca. $Fe_{10}O_{14}(OH)_2$. Birnessite $Na_xMn_{2-x}(IV)Mn(III)_xO_4$, x ~ 0.4, Goethite, α-FeOOH.